MULTICOLOR OBSERVATIONS OF THE GRB 000926 AFTERGLOW

P. A. PRICE,[1,2] F. A. HARRISON,[1] T. J. GALAMA,[1] D. E. REICHART,[1] T. S. AXELROD,[2] E. BERGER,[1] J. S. BLOOM,[1] J. BUSCHE,[3]
T. CLINE,[4] A. DIERCKS,[1] S. G. DJORGOVSKI,[1] D. A. FRAIL,[5] A. GAL-YAM,[6] J. HALPERN,[7] J. A. HOLTZMAN,[8]
M. HUNT,[1] K. HURLEY,[9] B. JACOBY,[1] R. KIMBLE,[4] S. R. KULKARNI,[1] N. MIRABAL,[7] G. MORRISON,[10]
E. OFEK,[6] O. PEVUNOVA,[10] R. SARI,[11] B. P. SCHMIDT,[2] D. TURNSHEK,[3] AND S. YOST[1]

ABSTRACT

We present multicolor light curves of the optical afterglow of gamma-ray burst (GRB) 000926. Beginning ~1.5 days after the burst, the light curves of this GRB steepen measurably. The existence of such achromatic breaks is usually taken to be an important observational signature that the ejecta are not expanding isotropically but rather have a collimated jetlike geometry. If we interpret the data in this context, we derive an opening angle of 5°, which reduces the energy release compared with an isotropic model by a factor of ~275, to 1.7×10^{51} ergs. To fit the data with a simple jet model requires extinction along the line of sight. The derived A_V is in the range 0.11–0.82 mag, depending on the adopted extinction law and whether the electrons giving rise to the optical emission are undergoing synchrotron cooling or not. Since this is in excess of the expected extinction from our Galaxy, we attribute this to the GRB host. We note that this extinction is typical of a galactic disk, and therefore the event likely took place in the disk of its host.

Subject headings: cosmology: observations — galaxies: ISM — gamma rays: bursts

1. INTRODUCTION

Multicolor light curves of the afterglows of gamma-ray burst (GRB) sources contain information about the evolution of the relativistic blast wave, which results from the progenitor explosion, as it expands into the surrounding medium. Interpreted in the context of a theoretical afterglow model (Sari, Piran, & Narayan 1998), the broadband light curve, if observed starting immediately after the GRB through the time when the shock becomes nonrelativistic, can, in principle, provide key physical parameters, including the total energy in the expanding ejecta, the density structure of the medium (Chevalier & Li 1999), and whether the ejecta are spherically symmetric or restricted to a jet (Rhoads 1997). The optical window of the afterglow spectrum is particularly useful for determining whether the ejecta are highly collimated, since it is generally well sampled on timescales of hours to days when temporal decay slope breaks due to this geometric effect become manifest. In addition, the effects of dust as seen through extinction are most easily observed in multicolor optical data.

Only about a half-dozen GRB afterglows have been well sampled in the optical, with data of sufficient quality to test

theoretical models and provide significant constraints on the physical parameters. In several cases, e.g., GRB 990510 (Stanek et al. 1999; Harrison et al. 1999), GRB 991216 (Halpern et al. 2000b), and GRB 000301c (Berger et al. 2000), the optical light curves exhibit achromatic breaks, most easily understood as resulting from jetlike ejecta collimated to angles of 5°, 6°, and 12°. The implied degree of collimation reduces the inferred energy release for these events by factors of 50–300. However, other events such as GRB 970508 show no evidence for collimation in the optical (but may in the radio; see Frail, Waxman, & Kulkarni 2000), indicating that the collimation angles are significantly larger.

In this letter, we present *BVRI* optical monitoring of the afterglow of GRB 000926 performed by the Palomar 60 and 200 inch, the MDM 2.4 m, and the Wise 1.0 m telescopes and derive the optical transient (OT) light curve from 1 to 7 days after the GRB. In addition, we have obtained high-resolution *Hubble Space Telescope* (*HST*)/WFPC2 images in several bands, which allow us to properly subtract the contribution from nearby diffuse emission, possibly associated with the GRB host. We have fitted the multicolor data with an afterglow model and find that observed steepening of the light curve requires the ejecta to be collimated in a cone. In the context of this model, consistency of the multicolor data and temporal decay also implies significant extinction, likely associated with the GRB host.

[1] Palomar Observatory, 105-24, California Institute of Technology, Pasadena, CA 91125.

[2] Research School of Astronomy and Astrophysics, Mount Stromlo Observatory, Cotter Road, Weston, ACT 2611, Australia.

[3] Department of Physics and Astronomy, University of Pittsburgh, Pittsburgh, PA 15260.

[4] Laboratory for Astronomy and Solar Physics, Code 681, Goddard Space Flight Center, Greenbelt, MD 20771.

[5] National Radio Astronomy Observatory, P.O. Box O, Socorro, NM 87801.

[6] School of Physics and Astronomy and Wise Observatory, Tel-Aviv University, Tel-Aviv 69978, Israel.

[7] Astronomy Department, Columbia University, 550 West 120th Street, New York, NY 10027.

[8] Department of Astronomy, New Mexico State University, Box 30001, Department 4500, Las Cruces, NM 88003-8001.

[9] University of California Space Sciences Laboratory, Berkeley, CA 94720.

[10] Infrared Processing and Analysis Center, 100-22, California Institute of Technology, Pasadena, CA 91125.

[11] Theoretical Astrophysics, 130-33, California Institute of Technology, Pasadena, CA 91125.

2. OBSERVATIONS AND DATA REDUCTION

GRB 000926 as observed by the Interplanetary Network (*Ulysses*, *Konus-Wind*, and *NEAR*) on 2000 September 26.993 UT had a duration of 25 s, placing it in the class of long-duration GRBs. The position was triangulated to a relatively small error box of approximately 35 arcmin² and distributed to the GRB community 0.84 days after the burst (Hurley et al. 2000a, 2000b). The bright ($R \sim 19.5$) afterglow of GRB 000926 was identified by Gorosabel et al. (2000) and Dall et al. (2000) from observations taken less than 1 day after the burst. Spectra of the afterglow from the Nordic Optical Telescope yielded an absorp-

OBSERVATIONS OF GRB 000926 AFTERGLOW

TABLE 1
GROUND-BASED MEASUREMENTS OF THE GRB 000926 OPTICAL
AFTERGLOW MADE AS A PART OF THIS WORK

Date (2000, UT)	Filter	Magnitude	Telescope
Sep 28.183	B	20.890 ± 0.038	MDM 2.4 m
Sep 28.188	B	20.967 ± 0.039	MDM 2.4 m
Sep 28.192	B	20.934 ± 0.043	Palomar 60 inch
Sep 28.202	B	20.874 ± 0.044	Palomar 60 inch
Sep 29.165	B	22.039 ± 0.071	Palomar 60 inch
Sep 29.178	B	21.979 ± 0.057	MDM 2.4 m
Sep 29.188	B	22.208 ± 0.074	MDM 2.4 m
Sep 29.214	B	22.22 ± 0.11	Palomar 60 inch
Sep 30.155	B	23.10 ± 0.12	Palomar 60 inch
Sep 30.183	B	23.126 ± 0.067	MDM 2.4 m
Oct 1.166	B	23.373 ± 0.091	Palomar 60 inch
Sep 28.737	V	21.25 ± 0.12	Wise 1.0 m
Sep 29.194	V	21.416 ± 0.063	Palomar 60 inch
Sep 29.234	V	21.573 ± 0.087	Palomar 60 inch
Sep 30.255	V	22.45 ± 0.33	Palomar 60 inch
Oct 3.138	V^{a}	23.726 ± 0.077	Palomar 200 inch
Sep 28.173	R	19.918 ± 0.020	MDM 2.4 m
Sep 28.178	R	19.890 ± 0.019	MDM 2.4 m
Sep 28.212	R	19.917 ± 0.033	Palomar 60 inch
Sep 28.221	R	19.902 ± 0.062	Palomar 60 inch
Sep 28.695	R	20.461 ± 0.093	Wise 1.0 m
Sep 29.155	R	20.985 ± 0.054	Palomar 60 inch
Sep 29.198	R	21.139 ± 0.043	MDM 2.4 m
Sep 29.204	R	21.028 ± 0.064	Palomar 60 inch
Sep 29.207	R	21.094 ± 0.041	MDM 2.4 m
Sep 29.243	R	21.118 ± 0.083	Palomar 60 inch
Sep 29.752	R	21.55 ± 0.15	Wise 1.0 m
Sep 30.189	R	21.906 ± 0.065	Palomar 60 inch
Sep 30.216	R	22.103 ± 0.057	MDM 2.4 m
Oct 1.195	R	22.56 ± 0.11	Palomar 60 inch
Oct 2.164	R	23.26 ± 0.19	Palomar 60 inch
Oct 2.172	R	23.235 ± 0.095	MDM 2.4 m
Oct 3.113	R^{b}	23.402 ± 0.063	Palomar 200 inch
Sep 28.172	I	19.359 ± 0.036	Palomar 60 inch
Sep 28.182	I	19.435 ± 0.096	Palomar 60 inch
Sep 29.199	I	20.230 ± 0.057	Palomar 60 inch
Sep 30.228	I	21.079 ± 0.083	Palomar 60 inch
Oct 1.247	I	22.51 ± 0.33	Palomar 60 inch

[a] This observation was made using a Sloan g' filter; Fukugita et al. 1996.

[b] This observation was made using an $\mathcal{R}$ filter; Steidel & Hamilton 1993.

tion redshift of 2.066 (Fynbo et al. 2000a), later refined to 2.0369 ± 0.0007 from Keck spectroscopy (Castro et al. 2000).

Our observations commenced with data taken by the MDM 2.4 m on September 28.177, 1.18 days after the burst. A complete log of our observations and resulting photometry can be found in Table 1. We used the $BVRI$ filter system for all observations save those with the Palomar 200 inch, for which observations were obtained in the $\mathcal{R}$ (Steidel & Hamilton 1993) and Sloan g' (Fukugita et al. 1996) filters.

We calibrated 12 secondary standards in the field from observations of Landolt (1992) standard star fields (Landolt fields 96, 112, 113, and 114). These fields were observed with the Palomar 60 inch telescope on two photometric nights. These observations are sufficient to fit extinction terms but not to extract a color term, which we took to be zero. From these standards and combined images of the field we also calibrated two fainter tertiary standards for use with larger telescopes. For the reference star of Halpern (2000a), we find $B = 18.468$, $V = 17.595$, $R = 17.048$, and $I = 16.512$. We estimate that these calibrations are accurate to approximately 3%.

The Palomar 200 inch telescope photometry was transformed to the $BVRI$ system using the published transformations (Steidel & Hamilton 1993; Fukugita et al. 1996) and OT colors of
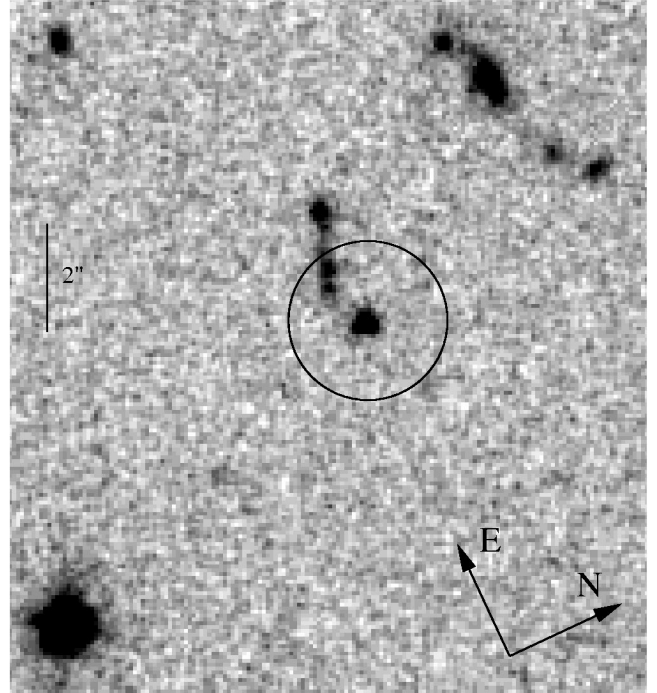

FIG. 1.—Combined *HST*/WFPC2 F606W image of the GRB 000926 optical afterglow. The extended emission approximately 1″.5 from the OT is the galaxy contaminating the ground-based measurements. The circle shows the aperture (1″.5) used for all our photometry.

$(B-V) = 0.61 \pm 0.10$ and $(R-I) = 0.75 \pm 0.10$. A 3% systematic error in the transformation was added in quadrature to the statistical error in these measurements. We compared magnitudes of field stars measured with the Palomar 60 inch telescope with transformed magnitudes from the 200 inch telescope photometry. This comparison suggests that our derived V and R magnitudes for the OT are accurate.

The I-band images display significant fringing, so the quoted formal errors do not represent the true measurement error. We estimated a systematic I-band error of 0.09 mag by fitting a straight line through the first four I-band measurements and adjusting the systematic error until χ^2/degrees of freedom (dof) = 1.

In addition to the ground-based photometric observations, we obtained high-resolution *HST*/WFPC2 images in F450W, F606W, and F814W at three epochs as part of a long-term monitoring program with *HST*. The 6600 s (three orbits) F450W images were combined using the STSDAS task "crrej," while the 13,200 s (six orbits) F606W and F814W images were combined and cosmic-ray rejected using the "drizzle" technique (Fruchter & Hook 1997). Figure 1 displays the resultant F606W image.

3. THE LIGHT CURVE

Both ground-based (Fynbo et al. 2000c) and *HST* (Fig. 1) imaging have revealed the presence of a galaxy near the OT, which contaminates photometry of the OT by ground-based telescopes. Proper treatment of this contamination is essential, since it can greatly influence the derived late-time slope and consequently the important physical parameters. For example, Rol, Vreeswijk, & Tanvir (2000) have fitted a late-time temporal slope of $\alpha_2 = 3.2 \pm 0.4$ for this afterglow, which is considerably steeper than that of other afterglows observed to date. We there-

TABLE 2

HST/WFPC2 Measurements of
Contaminating Galaxy Flux
within a 1″.5 Aperture
Centered on the OT

Band	Magnitude
B	26.23 ± 0.50
V	26.09 ± 0.16
R	25.19 ± 0.17
I	24.50 ± 0.11

fore use our *HST* images to measure the contaminating galaxy flux in a 1″.5 aperture from the OT and convert these to *BVRI* using Holtzman et al. (1995). The results are shown in Table 2. Our *R*-band measurement of the galaxy contribution is fainter than the fit value of Rol et al. (2000) of 24.2 ± 0.3, which may explain their steeper late-time slope.

In deriving flux values for all our ground-based data, we use a 1″.5 aperture. This allows us to accurately subtract the galaxy flux in a straightforward way, using the values tabulated above. We note that there may be an additional compact component of the host emission not resolved by *HST* (which may be observed in subsequent, scheduled observations). However, since the light curve shows no significant flattening, this is not likely to be an important contribution over the interval of our observations.

Since the aperture size used in measurements reported through the GRB Coordinate Network (GCN) circulars[12] is generally unspecified and variable, the amount of contamination by the galaxy in each measurement cannot be determined. Consequently, we include only measurements taken within 1 day of the GRB (Hjorth et al. 2000; Fynbo et al. 2000b), in addition to the measurements presented in this paper in constructing the light curve. These data are important for constraining the early-time temporal slope, and, at these times, the OT is bright and the contamination by the galaxy is negligible. The measurements from the GCN were recalibrated using our secondary standards. We correct all measurements for foreground Galactic extinction using $E_{B-V} = 0.023$ mag from Schlegel, Finkbeiner, & Davis (1998). In Figure 2 we display the OT light curve in which the contribution from the host galaxy has been subtracted and the Galactic reddening has been accounted for. A single power-law temporal decay is clearly excluded, with a probability that it fits the data of 3×10^{-6}.

In order to characterize the light curve, we have fitted it to the functional form (Beuermann et al. 1999)

$$F(t, \nu) = F_0 \nu^{\beta} [(t/t_*)^{-\alpha_1 s} + (t/t_*)^{-\alpha_2 s}]^{-1/s}. \qquad (1)$$

This function has no physical significance but provides a simple and general parametric description of the data, allowing for a gradual break in the afterglow decay. In this function, α_1 and α_2 are the early- and late-time asymptotic temporal slopes, respectively, t_* is the time of the temporal slope break, β is the spectral slope, and s is a parameter that determines the sharpness of the transition. We leave the break sharpness as a free parameter, since there is disagreement over its theoretical value (e.g., Kumar & Panaitescu 2000).

We first fitted equation (1) without any constraints, applying 5% systematic error (in addition to the errors given in Table 1 above) to all measurements to reflect uncertainties in zero-point

12 GCN circulars can be accessed from http://gcn.gsfc.nasa.gov/gcn/gcn3_archive.html.
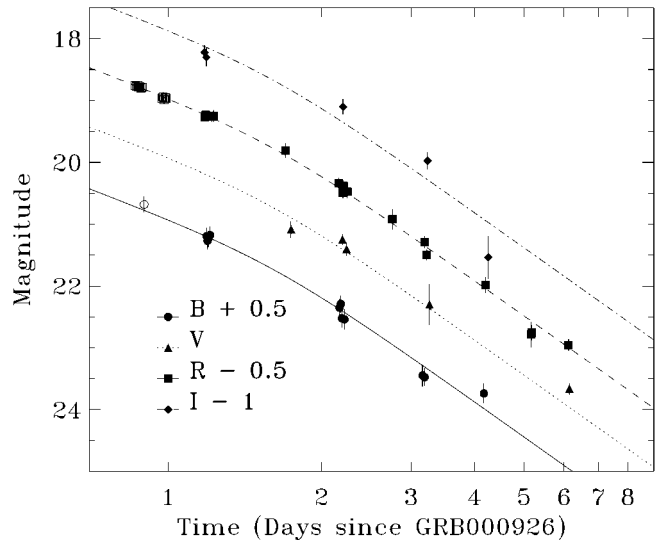

Fig. 2.—*BVRI* light curve of GRB 000926. Filled symbols are data presented in this work; open symbols ($t < 1$ day) are from Hjorth et al. (2000) and Fynbo et al. (2000b). The measurements have had the contaminating galaxy flux subtracted. The solid line shows the best fit to eq. (1).

calibrations for the different telescopes and in the conversion of WFPC2 magnitudes to *BVRI*. This form fits well, with $\chi^2/\text{dof} = 48.5/45$ and the fit parameters $t_* = 1.79 \pm 0.15$ days, $\alpha_1 = -1.48 \pm 0.10$, $\alpha_2 = -2.302 \pm 0.082$, and $\beta = -1.522 \pm 0.066$, where the errors do not reflect covariance between the parameters. The best-fit value for the break sharpness value is $s = 15$ but is not well constrained, because of the lack of early-time data. Figure 2 shows this fit overplotted on the data points.

4. INTERPRETATION

We have demonstrated that the observed break in the light curve is consistent with being achromatic, since the parameter t_* is independent of frequency. This frequency-independent steepening of the optical light curve is most easily interpreted as due to collimated, or jetlike, ejecta. Once the Lorentz factor of the ejecta falls below the inverse of the opening angle of the jet, the light curve steepens because of geometric effects, as well as because of the sideways expansion of the ejecta (Rhoads 1997, 1999). Interpreted in this context, the early- and late-time light-curve slopes, the optical spectral index, and the time of the transition constrain the index of the electron spectral energy distribution, p, the jet opening angle, and the total energy of the afterglow.

We now adopt the simple model developed by Sari et al. (1999). This model predicts the temporal and spectral evolution of synchrotron radiation from a jet expanding relativistically in a constant-density medium. The early- and late-time temporal slopes and the optical spectral slope are determined by the electron spectral index, p, and the break time is determined by the jet opening angle. Optical data alone do not have sufficient frequency coverage to locate all of the afterglow spectral breaks. Specifically, with the optical light curve we cannot constrain the position of the cooling break, ν_c, and we must consider two cases: (1) ν_c is blueward of the optical (hereafter referred to as "case B"); and (2) ν_c is redward of the optical (hereafter "case R").

We find that, when we fit light curves from all optical bands

simultaneously (linking the spectral slope and the two temporal decay slopes) using the theoretical predictions of the model, we cannot produce an acceptable fit to the data. Our χ^2-values of 195 and 83 for 47 dof for case B and case R, respectively, correspond to a probability that the model describes the data of less than 2×10^{-4}. Clearly, the observed optical spectral index is inconsistent with the model, being too steep for the value of p determined from the temporal decay slopes.

This problem can be resolved if we include the effect of extinction in the host galaxy of the GRB, which can modify the spectral index. This explanation is consistent with the strong equivalent widths of absorption lines observed in spectra of this afterglow from the Keck telescope (Castro et al. 2000). The appropriate extinction law is, however, unknown and unconstrained by our data, so to determine the source frame A_V we consider several possibilities. We allow for extinction laws corresponding to young star-forming regions (such as the Orion Nebula), the Milky Way, the LMC, and the SMC by using the Cardelli, Clayton, & Mathis (1989) and the Fitzpatrick & Massa (1988) extinction curves, with the smooth joining calculated by Reichart (1999).

Including extinction provides an acceptable fit to the multiband data for both cases, with an electron energy spectral index $p = 2.38 \pm 0.15$, which is consistent with that found for other afterglows. For case B, the derived A_V-values range from 0.82 mag for the Milky Way extinction law to 0.28 and 0.25 mag for the LMC and the SMC extinction laws ($\chi^2 \approx 50$ for 46 dof), with a break time of $t_* = 1.45 \pm 0.14$ days. For case R, A_V is 0.36/0.12/0.11 for Milky Way/LMC/SMC extinction, with a break time of $t_* = 1.60 \pm 0.13$ days. In both cases, an extinction law corresponding to a young star-forming region does not fit the data, since it is "gray" in the source-frame UV.

The parameter p is insensitive to the extinction law and the position of the cooling break to within the quoted error. We calculate the corresponding jet half-opening angle using Sari et al. (1999) to be $\theta_0 \sim 5° n_1^{1/8}$, where n_1 is the density of the ISM, in units of cm^{-3}.

5. CONCLUSIONS

Our well-sampled multicolor light curve of the afterglow of GRB 000926 is well described by a physical model where the ejecta are collimated in a jet. The degree of collimation reduces the inferred isotropic radiated energy of the GRB (Bloom et al. 2001) by a factor of 275, to $1.7 \times 10^{51} n_1^{1/4}$ ergs. This inferred energy release is typical of events observed to date. Furthermore, we find that, in order to properly fit the light curve of this afterglow, extinction is required. Assuming the extinction is at the measured redshift of $z = 2.0369$ (Castro et al. 2000), we can exclude an extinction law corresponding to a young star-forming region, and we find an A_V ranging from 0.11 to 0.82 mag, depending on the assumed curve and on the cooling regime. This value exceeds the expected extinction from our own Galaxy and is likely due to the host galaxy of the GRB.

REFERENCES

Berger, E. J., et al. 2000, ApJ, 545, 56
Beuermann, K., et al. 1999, A&A, 352, L26
Bloom, J. S., et al. 2001, AJ, in press (astro-ph/0102371)
Cardelli, J. A., Clayton, G. C., & Mathis, J. S. 1989, ApJ, 345, 245
Castro, S. M., Djorgovski, S. G., Kulkarni, S. R., Bloom, J. S., Galama, T. J., Harrison, F. A., & Frail, D. A. 2000, GCN Circ. 851
Chevalier, R. A., & Li, Z.-Y. 1999, ApJ, 520, L29
Dall, T., Fynbo, J. P. U., Pedersen, H., Jensen, B. L., Hjorth, J., & Gorosabel, J. 2000, GCN Circ. 804
Fitzpatrick, E. L., & Massa, D. 1988, ApJ, 328, 734
Frail, D., Waxman, E., & Kulkarni, S. R. 2000, ApJ, 537, 191
Fruchter, A. S., & Hook, R. N. 1997, Proc. SPIE, 3164, 120
Fukugita, M., Ichikawa, T., Gunn, J. E., Doi, M., Shimasaku, K., & Schneider, D. P. 1996, AJ, 111, 1748
Fynbo, J. P. U., Moller, P., Dall, T., Pedersen, H., Jensen, B. L., Hjorth, J., & Gorosabel, J. 2000a, GCN Circ. 807
Fynbo, J. P. U., Moller, P., Gorosabel, J., Hjorth, J., Jensen, B. L., & Pedersen, H. 2000b, GCN Circ. 825
Fynbo, J. P. U., et al. 2000c, GCN Circ. 840
Gorosabel, J., Castro Ceron, J. M., Castro-Tirado, A. J., Greiner, J., Wolf, C., & Lund, N. 2000, GCN Circ. 803

Halpern, J. P., Mirabal, N., Turnshek, D., & Busche, J. 2000a, GCN Circ. 806
Halpern, J. P., et al. 2000b, ApJ, 543, 697
Harrison, F. A., et al. 1999, ApJ, 523, L121
Hjorth, J., Jensen, B. L., Pedersen, H., Fynbo, J. U. P., Moller, P., & Gorosabel, J. 2000, GCN Circ. 809
Holtzman, J. A., Burrows, C. J., Casertano, S., Hester, J. J., Trauger, J. T., Watson, A. M., & Worthey, G. 1995, PASP, 107, 1065
Hurley, K., Mazets, E., Golenetskii, S., & Cline, T. 2000a, GCN Circ. 801
———. 2000b, GCN Circ. 802
Kumar, P., & Panaitescu, A. 2000, ApJ, 541, L9
Landolt, A. U. 1992, AJ, 104, 340
Reichart, D. E. 1999, ApJ, in press (astro-ph/9912368)
Rhoads, J. E. 1997, ApJ, 487, L1
———. 1999, ApJ, 525, 737
Rol, E., Vreeswijk, P. M., & Tanvir, N. 2000, GCN Circ. 850
Sari, R., Piran, T., & Halpern, J. 1999, ApJ, 519, L17
Sari, R., Piran, T., & Narayan, R. 1998, ApJ, 497, L17
Schlegel, D. J., Finkbeiner, D. P., & Davis, M. 1998, ApJ, 500, 525
Stanek, K. Z., Garnavich, P. M., Kaluzny, J., Pych, W., & Thompson, I. 1999, ApJ, 522, L39
Steidel, C. C., & Hamilton, D. 1993, AJ, 105, 2017